14TH CANADIAN MASONRY SYMPOSIUM
MONTREAL, CANADA
MAY 16TH – MAY 20TH, 2021

DEPENDENCY OF THE COMPRESSIVE STRENGTH OF CONCRETE MASONRY ON PRISM'S SIZE

Abasi, Ali[1]; Hassanli, Reza[2]; Vincent, Thomas[3] and Manalo, Allan[4]

ABSTRACT

Variation in the size of test prisms can affect the measured compressive strength of concrete masonry and result in unsafe overprediction. Thus, current masonry codes provide correction factors to modify the strength by considering the height-to-thickness ratio of the prism. This study investigated the accuracy of the available correction factors and methods provided in masonry codes, and examined the effects of the length-to-thickness ratio as well as the height-to-thickness ratio of prisms on the compressive strength. The numerical study was conducted based on the finite element method and verified against different experimental tests. The results show that, in addition to the height-to-thickness ratio, the length-to-thickness ratio plays an important role in the compressive strength of the prisms and should be considered in estimating the compressive strength of masonry prisms.

KEYWORDS: *compressive strength, concrete masonry, correction factors, finite element method, height-to-thickness ratio, length-to-thickness ratio*

[1] Ph.D. student, Department of Civil and Environmental Engineering, Western University, London, ON, Canada. Email: aabasi@uwo.ca.
[2] Lecturer, School of Natural and Built Environments, University of South Australia, Mawson Lakes, SA 5095, Australia. Email: reza.hassanli@unisa.edu.au.
[3] Senior Lecturer, College of Science and Engineering, Flinders University, Bedford Park, SA 5042, Australia. Email: thomas.vincent@flinders.edu.au.
[4] Professor, Center for Future Materials, Faculty of Health, Engineering and Sciences, Univ. of Southern Queensland, Toowoomba, QLD 4350, Australia. Email: allan.manalo@usq.edu.au.

INTRODUCTION

Masonry is one of the most common structural materials, and its strength depends on the properties of its components, including unit, mortar, and their interaction [1, 2]. There are two methods to determine the compressive capacity of masonry prisms, A) Experimentally testing of masonry prisms, and B) Using the strength of masonry unit and mortar and estimate the strength using code's defined tables. To accurately measure the compressive strength of masonry, which is a critical parameter for design, experimental tests are conducted using a compressive testing machine that contains two platens. These platens impose friction to the top and bottom faces of the prisms, which causes lateral confinement at the prism ends. The impact of lateral confinement does not influence the prisms' compressive strength if their height is large enough with respect to other dimensions. However, most compression test machines cannot accommodate tall prisms such as five-course concrete masonry. Hence, the masonry codes consider the results of smaller size prisms together with a correction factor to normalize the compressive strength of the concrete masonry prisms based on the height-to-thickness (*h/t*) ratio [3-5].

The ratio of compressive strength of a reference prism to a test prism is defined as the correction factor. Some masonry codes such as CSA S304 [5] and AS 4456 [3] consider a prism with the *h/t* of five as the reference prism for all types of masonry; but ASTM C1314 [4] defines the reference prism as two-course for concrete and five-course for clay masonry. According to existing research, it can be expected that the strength of short prisms, such as the two-course concrete prism, may be affected by the lateral confinement, which causes overprediction of the compressive strength. Comprehensive experimental studies on concrete masonry indicated that the masonry code recommendations lead to an overestimation of the compressive strength [6]. Besides, it was showed that the correction factors recommended in CSA S304 [5] lead to overestimation in the compressive strength of hollow masonry [7].

ASTM C1314 [4] allows the compressive strength of prisms to be obtained by experimentally testing half-block or full-block size prisms. So, the impacts of the prism's length are not considered as a factor contributing to the strength, and this was not studied in previous research studies. Hassanli et al. [8] and Abasi et al. [9] examined the effects of prism's dimensions, including length-to-thickness *(l/t*) and *h/t* ratios on the compressive strength of the concrete prisms, and recommended correction factors for prisms with different sizes. Hassanli et al. [8] used macro-modeling finite element (FE) method; however, the simplified-micro-modeling method was used in this study.

As there are limited researches in this field, in this paper, a micro-modeling FE approach was used to investigate the effects of the length of prisms on their compressive strength. FE models of masonry prisms were first developed and calibrated then verified against different sets of experimental results. Next, a comprehensive parametric study on prisms with different sizes was conducted. The effects of various parameters are discussed, and new correction factors are proposed to convert the masonry strength to a standard size reference masonry prism by considering the effects of the both *l/t* and *h/t* ratios.

FINITE ELEMENT (FE) SIMULATION

There are two main FE analysis methods for masonry components including macro-modeling and micro-modeling method (which includes detailed-micro-modeling, and simplified-micro-modeling) [12]. In the macro-modeling method, which is convenient and gives conservative results, mortar layers are not modeled. On the other hand, masonry units and mortar layer simulated in micro-modeling method. In this study, simplified-micro-modeling approach was utilized, where the mortar layer was defined as a zero-thickness element (planar element), however the units were simulated as a 3D element (the C3D8R element), and they were extended to cover half of the mortar thickness [12]. The cohesive surface-based element was applied as the interaction of units to simulate the effects of the mortar in ABAQUS. Displacement control approach was considered where displacements were applied with the rate of 0.001 mm/s. Moreover, the top and bottom nodes were fully restrained in the lateral directions as the boundary conditions, to simulate the prism's friction at the platens' interface.

Two types of blocks, including grouted and un-grouted, have been considered in this paper for model verification, and masonry units in the all prisms in this study were established based on stack bond pattern. The geometry of the grouted and un-grouted blocks were $406 \times 203 \times 203$ mm (Length (l) $\times$ Height (h) $\times$ Thickness (t)) and $406 \times 203 \times 101$ mm, respectively. Material properties of the prisms are presented in Table 1 based on the results of tests, conducted by Bolhassani et al. [13]. The Concrete Damage Plasticity model (CDP), which is suitable for concrete and other brittle material [14], is used in this research as the constitutive model. In addition to the range of yield stress and its corresponding inelastic strain, the CDP model depends on five main parameters, which are discussed in detail in the following sections. The range of yield stress and their corresponding inelastic strain for both tension and compression damages of the prisms were adopted from tests conducted by Bolhassani et al. [13], and were used for FE simulation in this study (Table 2).

Table 1. Material properties of the prisms.

Prism [13]	Compressive strength (MPa)	Tensile strength (MPa)	Modulus of elasticity (GPa)	Poisson's ratio
Three-course-grouted	21.60	1.50	33.70	0.2
Three-course un-grouted	17.90	0.64	26.20	0.2

Table 2. Plastic behavior of the material of the three-course-grouted and un-grouted prisms [13].

Three-course-grouted prism				Three-course un-grouted			
Compressive behavior		Tensile behavior		Compressive behavior		Tensile behavior	
Yield stress (MPa)	Inelastic strain	Yield stress (MPa)	Cracking strain	Yield stress (MPa)	Inelastic strain	Yield stress (MPa)	Cracking strain
17.4	0	1.5	0	13.8	0	0.64	0
20.7	0.0003	1.15	0.0003	17.2	0.00012	0.62	0.00006
21.6	0.0005	0.83	0.0004	17.9	0.00032	0.34	0.00028
20.9	0.001	0.3	0.0009	13.8	0.00057	0.21	0.00045
19.6	0.0015	0.1	0.003	7.6	0.00131	0.12	0.00079
15.1	0.0029	0.06	0.0045	4.4	0.00191	0.05	0.00139
10.3	0.0045	0.05	0.005	2.2	0.00245	0.03	0.00299
2	0.0099	-	-	1	0.00295	0.02	0.00349

The cohesive interaction is used as the interaction of units, which can be defined in the traction–separation constitutive model, and it can be simulated as the surface-to-surface contact in ABAQUS. Table 3 shows the cohesive behavior of the interaction joints of the three-course-grouted and un-grouted prisms based on the tests conducted by Bolhassani et al. [13]. Hard-Contact behavior was assumed between the units to prevent the penetration of elements.

Table 3. Properties of cohesive interaction [13].

Prism	**Tangential behavior**	**Normal behavior**	**Cohesive behavior**						
			Stiffness coefficients (MN/m)			**Damage initiation (MPa)**			**Damage evolution**
	Friction coefficient	Type	K_{nn}	K_{ss}	K_{tt}	Normal	Shear I	Shear II	Plastic displacement (mm)
Three-course grouted	0.78	Hard contact	14	14	0	23.70	0.60	0	2.30
Three-course un-grouted	0.78	Hard contact	8.70	8.70	0	12.60	0.21	0	2.00

Mesh sensitivity analysis

The results of the FE analysis depend on the mesh size of elements. Figure 1 shows the results of the mesh sensitivity analysis for the three-course-grouted prism. The mesh sensitivity analysis shows that a mesh density (the ratio of the number of the elements to the area) of more than 600 does not affect the results considerably. Hence, a mesh size of 35 mm (density of 870) was chosen in all the simulations presented in this study.

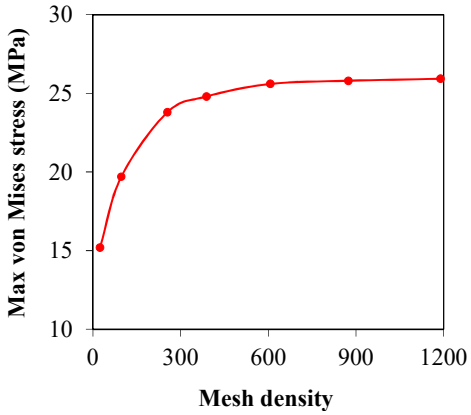

Figure 1. Mesh-sensitivity analysis of the FE model of the three-course-grouted prism.

CALIBRATION AND VERIFICATION OF THE FE MODEL

Calibration of CDP parameters

The CDP model depends on five parameters, including dilation angle (Ψ), eccentricity (e), f_{b0}/f_{c0} ratio, shape factor (k), and viscosity. The effects of these parameters were examined against the experimental results of the three-course-grouted prism conducted by Bolhassani et al. [13] to calibrate the material properties. Due to the relatively inelastic behavior of brittle materials, considerable volume change can occur, which is commonly referred to as dilatancy [15]. Various dilation angle values including 30°, 32°, 34°, and 45° have been used in previous studies on concrete masonry [13, 14, 16, 17]. In this study, the dilation angles ranging from 30° to 45° were examined to investigate the impacts of the dilation angle on the behavior of prisms (Figure 2a). As shown, there is no noticeable differences between the behavior of masonry prisms having different dilation angles, because this parameter affects the shear plastic behavior and shear distortion of the FE models [18], not compressive behavior. This similarity in behavior can be attributed to the pure compression failure mode of prisms subjected to only axial load. Considering Figure 2a and the recommendations provided in the previous studies, a dilation angle of 34° was adopted in this study.

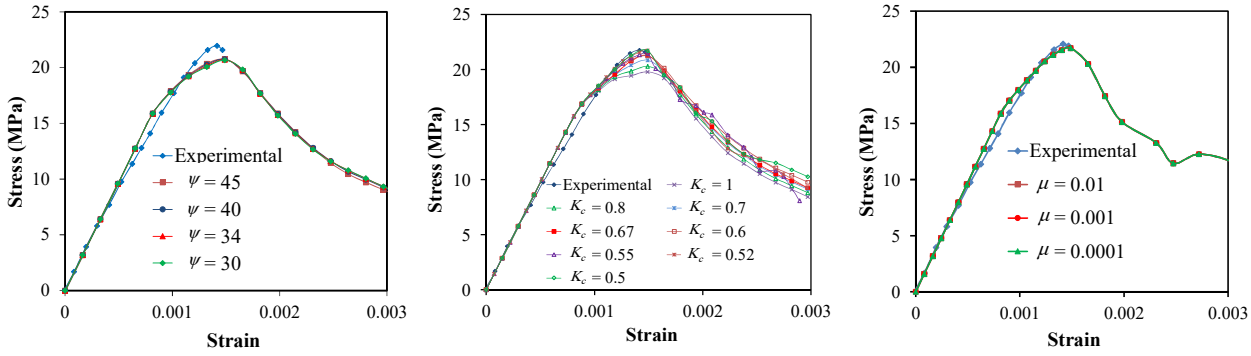

Figure 2. The stress-strain curves of the FE models with different values of the CDP parameters; (a) dilation angle, (b) shape factor, (c) viscosity parameter.

Shape factor (K_c) is defined as the ratio of the tensile to the compressive meridian, which describes the shape of the yield surface in the deviatory surface [18]. K_c can range from 0.5 to 1.0, and a K_c of 0.67 has been recommended in many previous studies for concrete masonry [13, 14, 16, 17]. In this study, a K_c varying between 0.5 and 1.0 was used to examine its effects. As can be seen in Figure 2b, as the K_c increases, the peak strength decreases. However, for K_c of less than 0.67, it does not have a considerable effect. As a K_c of 0.67 is recommended and commonly used in the previous studies, this value was adopted in this research. f_{b0}/f_{c0} is the ratio of the biaxial compressive strength of the material to its uniaxial compressive strength. Flow potential eccentricity (e) is a parameter that defines the rate at which the hyperbolic flow potential approaches its asymptote [18]. Considering it is well established that $f_{b0}/f_{c0} = 1.16$ and $e = 0.1$ for concrete masonry [13, 14, 16-19], these values were adopted in this study.

Viscosity parameter (μ) represents the relaxation time of the viscoplastic system. The viscosity parameters of 0.01, 0.001, and 0.0001 are recommended in previous studies for concrete masonry [13-17], and these values were examined in this paper (Figure 2c). The viscosity parameter can improve the rate of analysis convergence, but, as shown, it does not impose considerable impacts on the behavior of brittle materials such as concrete in monotonic loading cases. Considering this, a viscosity of 0.001 was selected for concrete masonry, as used frequently in previous similar studies. The values of the calibrated material model used in the simulation was as follows: μ=0.001, e= 0.10, f_{b0}/f_{c0}=1.16, K_c= 0.67, and ψ=34°. The stress-strain response of the calibrated numerical model is plotted against experimental results (Figure 3- three-course-grouted prism). As shown, the model can accurately predict the peak strength, within 1.1% error, as well as stiffness and general stress-strain behavior.

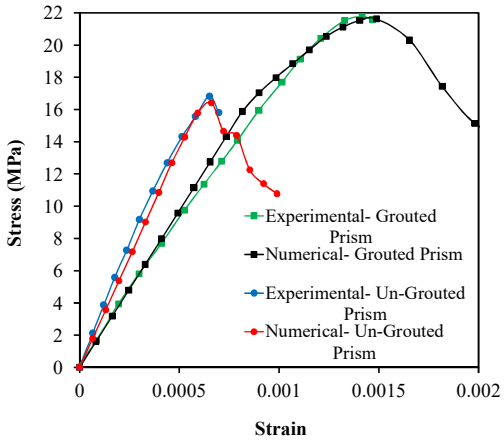

Figure 3. The experimental and numerical stress-strain curve of the three-course-grouted and un-grouted prisms.

Verification of the FE model

The results of the verifications of the calibrated material model against the three-course un-grouted prism are shown in Figure 3. As shown, the numerical results are in good agreement with the

experimental data, and stiffness and peak strength as well as stress-strain behavior were produced accurately using the FE models. The verified FE model is used in the following sections.

PARAMETRIC STUDY

Several FE models were implemented in this section to investigate the effects of *h/t* and *l/t* on the compressive behavior of concrete masonry prisms. The parameters calibrated in the previous section and the same material properties of the three-course-grouted prism were used here, and all FE models were simulated based on a stacked pattern of the masonry units.

Effect of support confinement

To investigate the influences of the friction on the compressive behavior, two-course and five-course prisms were analyzed. Both prisms had a thickness of 203 mm, lengths of 406 mm and were simulated twice: A) assuming frictionless ends, and B) assuming restrained ends due to the friction. Their axial stress contours at their peak strength due to the axial loading are displayed in Figure 4. As shown, the prisms with friction at specimen ends experienced a larger range of stresses. The ranges of stress for the two-course prisms with restrained and frictionless ends (Figure 4a and 4b) were 18.51 MPa (from 18.93 to 37.44 MPa) and only 0.03 MPa (from 19.54 to 19.57 MPa), respectively. As expected, by removing friction at the prism ends, the axial stresses distribute more uniformly within the entire prism regardless of its height (Figure 4b and 4d). The axial stress distribution at specimen mid-height during peak strength of the prisms is summarized in Figure 5.

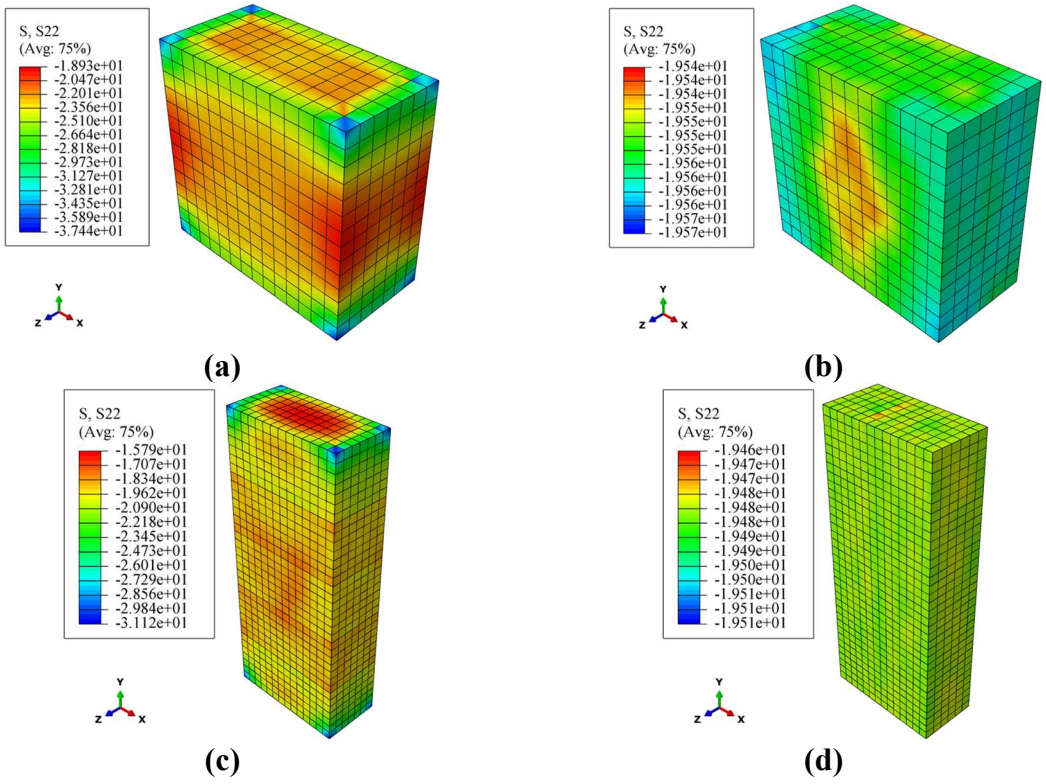

Figure 4. Axial stress distribution at the peak strength of the prisms; (a) two-course prism with restrained ends, (b) two-course prism with frictionless ends, (c) five-course prism with restrained ends, and (d) five-course prism with frictionless ends.

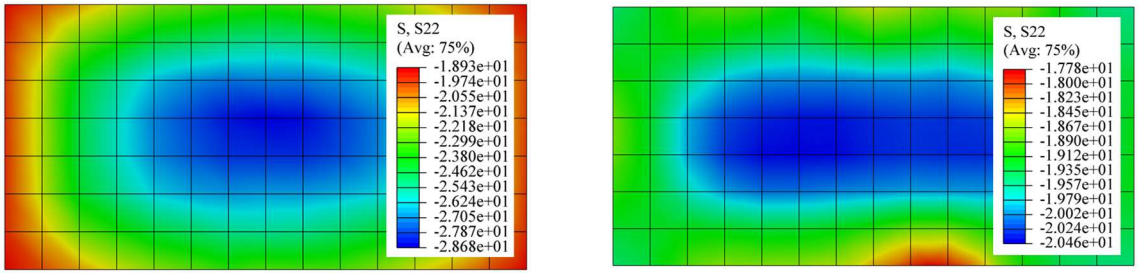

(a) **(b)**

Figure 5. Axial stress distribution at specimen mid-height during peak strength of prisms; (a) two-course prism with restrained ends and (b) five-course prism with restrained ends.

The two-course prism with restrained ends (Figure 5a) have a noticeably higher variation in stress distribution at the middle and corner elements at the mid-height section when compared to the five course prism with restrained ends (Figure 5b). Considering this, as the height of prisms increases, the effects of prism end friction on the stress distribution and compressive strength of prisms decreases.

Effects of the prism length

A comparison of the transverse stress distribution for 203 mm prisms at their peak strength with two, three, and five courses constructed using half, full and double blocks is shown in Figure 6, to investigate the effects of prism length as well as height on the compressive behavior. The *l/t* ratio of the half, full and double blocks were one, two, and four, respectively, and all prisms were modelled in the form of stacked pattern. All prisms were simulated with restrained ends. As can be seen, as the prism height increases, the effect of prism end friction on the mid-height section of the prism increases (see Figure 6b, 6e, and 6h). Moreover, if the height of the prism is significantly large, the effect of end friction on elements at the mid-height section is negligible. This can be seen in Figure 6g, 6h, and 6i, which show that the effect of friction on the behavior of five-course prisms is insignificant, regardless of the block length. Therefore, a prism with $h/t = 5$ should be considered as the reference prism to obtain the correction factors. Some codes, such as ASTM C1314 [4], consider a prism with $h/t = 2$ as the reference prism for concrete masonry, which leads to overprediction of the strength of the concrete masonry.

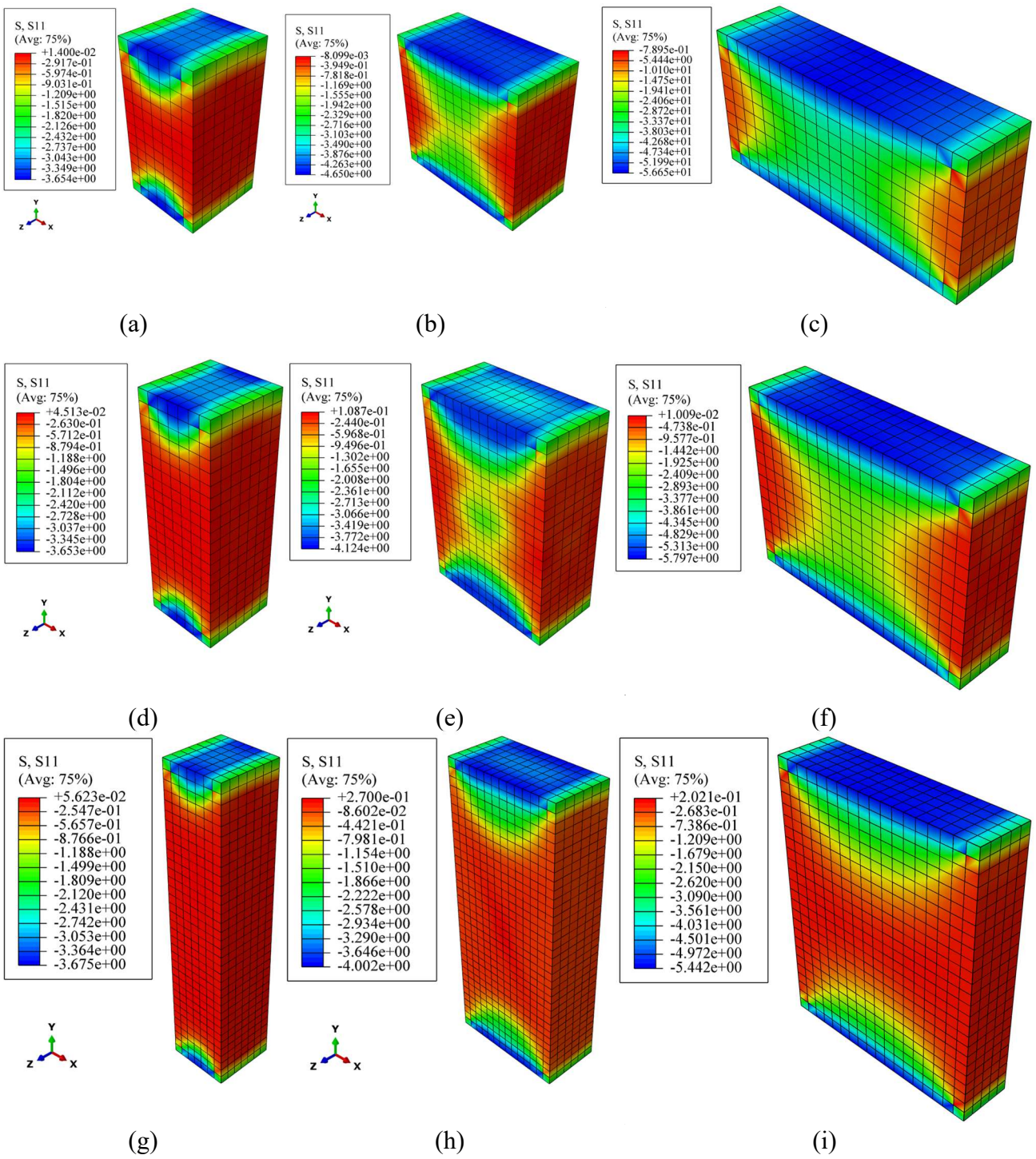

Figure 6. Transverse stress distribution at the peak strength for the prisms with restrained ends; (a) two-course half-block, (b) two-course full-block, (c) two-course double-block, (d) three-course half-block, (e) three-course full-block, (f) three-course double-block, (g) five-course half-block, (h) five-course full-block, and (i) five-course double-block prism.

Figure 6 also illustrates that as the prism length increases, the effect of prism end friction on the mid-height section of the prism increases (see Figure 6d, 6e, and 6f), which result in an unsafe

overprediction of strength prediction. Hence, in addition to the height of prisms, the prism length has a considerable impact on compressive strength of specimens. Accordingly, new correction factors, which consider both *h/t* and *l/t* ratios, should be used in the design of concrete masonry structures.

CORRECTION FACTORS

The new correction factors for masonry prisms considering the effects of both *h/t* and *l/t* were proposed in this section. The compressive strengths of the 203 mm prisms, having different lengths and heights, are normalized by the strength of the corresponding five-course prism and are shown in Table 4. The correction factors of some masonry codes including ASTM C1314 [4], AS 4456.4 [3], and CSA S304-14 [5], are also presented here. The correction factors of ASTM C1314 [4] are normalized for $h/t = 5$ to be compatible, because a two-course prism ($h/t = 2$) is considered as the reference prism in this code, in contrast to the other masonry codes.

According to Table 4, as *l/t* decreases, the correction factors increase. Besides, the correction factors provided in all presented codes, apart from ASTM C1314 [4], are in good agreement with the results for full-block prisms. However, when it comes to half-block prisms, the correction factors are higher than those presented in the codes. This implies that by using half-block prisms (ASTM C1314 [4]), the strength of the masonry prisms is underestimated. On the other hand, the strength of prisms obtained from larger *l/t* ratios such as double-block prisms are overestimated, which can result in under-designed masonry structures.

Table 4. Correction factors for 203 mm prism.

Number of courses	*h* (mm)	*t* (mm)	Strength (MPa)			*h/t* ratio	Correction factors			AS4456.4	ASTM C1314	ASTM C1314 (normalized)	CSA S304.1
			Double-block	Full-block	Half-block		Double-block	Full-block	Half-block				
One	203	203	38.70	35.98	31.77	1.00	0.50	0.54	0.61	0.70	-	-	-
Two	406	203	25.40	22.66	21.27	2.00	0.77	0.86	0.92	0.81	1.00	0.82	0.80
Three	609	203	23.61	21.72	20.44	3.00	0.83	0.89	0.95	0.89	1.07	0.88	0.90
Four	812	203	21.69	20.39	19.87	4.00	0.90	0.96	0.98	0.95	1.15	0.94	0.95
Five	1015	203	19.50	19.50	19.50	5.00	1.00	1.00	1.00	1.00	1.22	1.00	1.00

Based on Table 4, five course prisms with different length have the equal compressive strength of 19.50 MPa, which implies that a five-course prism can be considered as the reference specimen to obtain correction factors regardless of the prism length. The proposed correction factors are summarized in Table 5. For a prism with a *h/t* and/or *l/t* different from the values presented in Table 5, linear interpolation can be used to obtain a correction factor. Note that the proposed correction factors have been developed for grouted prisms, and similar investigations is required for un-grouted prisms to develop such correction factors.

Table 5. Proposed correction factors.

	h/t= 1	*h/t*= 2	*h/t*= 3	*h/t*= 4	*h/t*= 5
***l/t*> 4**	0.50	0.77	0.83	0.90	1.00
***l/t*= 2**	0.54	0.86	0.89	0.96	1.00
***l/t*= 1**	0.61	0.92	0.95	0.98	1.00

DISCUSSION

Complementary tests were also conducted to verify the concept of the effect of the *l/t* ratio on the prisms' strength. To filter out the effect of mortar layer, three half-length and three full-length grouted units were tested, and their results are presented in Table 6. Due to premature failure of one of the full-length specimens, its results were removed. The strength of full-length specimen as can be seen in Table 6 is almost 20% higher than that of the half-length specimen, that confirm the effectiveness of the *l/t* ratio on the strength of masonry.

Table 6. Compression test results.

Specimen	*t (mm)*	*l (mm)*	*l/t*	Strength (MPa)
Half-block	195	212	1.1	21.70
	195	213	1.1	23.73
	196	210	1.1	19.36
Full-block	194	397	2.0	25.82
	194	397	2.0	26.00

CONCLUSION

A comprehensive numerical study was implemented to examine the impacts of prisms' size on their compressive strength. The results show that for prisms with *h/t* of less than five, confinement at the top and bottom of the prisms leads to overestimating the compressive strength of short masonry prisms. For prisms with *h/t* of five or more, no influence of end confinement is observed, regardless of the *l/t* ratio. In addition to the *h/t* ratio, the *l/t* ratio has significant effects on the strength of masonry prisms. Thus, it is strongly suggested that the correction factors in masonry codes be revised to account for the effect of *l/t* ratio. New correction factors have been recommended in this study within the range of 1 to 5 for *h*/*t* and 1 to 4 for *l*/*t*.

REFERENCES

[1] Ravula, M.B. and Subramaniam K.V. (2017). "Experimental investigation of compressive failure in masonry brick assemblages made with soft brick." *Materials and Structures*, 50(1): p. 19.

[2] Dunphy, K., Sadhu, A., and Banting, B. (2021). "Experimental and numerical investigation of tensile properties of early-age masonry." *Materials and Structures*, 54, 40.

[3] *AS 4456.4: Methods of Determining Compressive Strength of Masonry Units*, (2003). Standards Australia: Sydney, Australia.

[4] *ASTM C1314-18: Standard Test Method for Compressive Strength of Masonry Prisms*, (2018), ASTM International: West Conshohocken.

[5] Association, C.S. (2014). *CSA S304-14: Masonry design of buildings.* CSA, Mississauga, ON, Canada.
[6] Sarhat, S.R. and Sherwood E.G. (2014). "The prediction of compressive strength of ungrouted hollow concrete block masonry." *Construction and Building Materials*, 58: p. 111-121.
[7] Das, S., et al. (2013). "Effect of height-to-thickness ratio on compressive Strength of hollow concrete masonry." *12th Canadian masonry symposium (CMS 2013)*, Vancouver, Canada.
[8] Hassanli, R., ElGawady, M.A., and Mills, J.E. (2015). "Effect of dimensions on the compressive strength of concrete masonry prisms." *Advances in Civil Engineering Materials*, 4(1): p. 175-201.
[9] Abasi, A., et al. (2020). "Influence of prism geometry on the compressive strength of concrete masonry." *Construction and Building Materials*, 264: p. 120182.
[10] Soraghi, A., and Huang, Q. (2021). "Probabilistic prediction model for RC bond failure mode." *Engineering Structures*, 233, 111944.
[11] Rahai, A., and Abasi A. (2018). "Seismic performance and long-term behavior of balanced cantilever light-weight concrete bridges." *6th European Conference on Earthquake Engineering (16ECEE)*, Thessaloniki, Greece.
[12] Abdulla, K.F., Cunningham, L.S., and Gillie, M. (2017). "Simulating masonry wall behaviour using a simplified micro-model approach." *Engineering Structures*, 151: p. 349-365.
[13] Bolhassani, M., et al. (2015). "Simplified micro modeling of partially grouted masonry assemblages." *Construction and Building Materials*, 83: p. 159-173.
[14] Mohamad, A.-B.A.E., and Chen, Z. (2016). "Experimental and numerical analysis of the compressive and shear behavior for a new type of self-insulating concrete masonry system." *Applied Sciences*, 6(9): p. 245.
[15] Genikomsou, A.S. and Polak, M.A. (2015). "Finite element analysis of punching shear of concrete slabs using damaged plasticity model in ABAQUS." *Engineering Structures*, 98: p. 38-48.
[16] Bolhassani, M., Hamid, A., and Moon, F. (2016). "Enhancement of lateral in-plane capacity of partially grouted concrete masonry shear walls." *Engineering Structures*, 108: p. 59-76.
[17] Dauda, J., Iuorio, O., and Paulo, L. (2018). "Characterization of Brick Masonry: Study towards Retrofitting URM Walls with Timber-Panels." *10th International Masonry Conference (10thIMC)*, Milan, Italy.
[18] Hibbitt, H., Karlsson, B., and Sorensen, P. (2016). *"Abaqus analysis user's manual version 2016."* Dassault Systèmes Simulia Corp, Providence.
[19] Dere, Y. and Koroglu, M.A. (2017). "Nonlinear FE modeling of reinforced concrete." *International Journal of Structural and Civil Engineering Research*, 6(1): p. 71-74.